

PACS numbers: 42.60.Da; 42.60.Fc
DOI: 10.1070/QE2011v041n07ABEH014341

Effect of complex recovery of saturable absorption on the performance of mode-locked lasers

O.G. Okhotnikov, R. Herda

Abstract. **Saturable absorbers with balanced slow and fast recovery mechanisms exhibiting a broadband recovery dynamics are shown to be advantageous for both reliable start-up of passive mode-locking and efficient pulse shortening.**

Keywords: *quantum-confined semiconductors, semiconductor nonlinear optics, semiconductor saturable absorber mirror (SESAM), mode-locking.*

1. Introduction

Semiconductor saturable absorbers are proven to be the key components for short pulse generation by passively mode-locked solid-state, semiconductor and fibre lasers. Based on mature semiconductor technologies [molecular beam epitaxy (MBE) or metalorganic chemical vapour deposition (MOCVD)], semiconductor absorbers offer flexible tailoring of optical parameters and simplicity of the light coupling, fibre pigtailing and polarisation insensitivity.

It should be noted that semiconductor absorbers can exhibit both fast and slow temporal components in the recovery dynamics. These components originate from the intraband and band-to-band transitions and influence the start-up of mode-locking and pulse shaping process. Though the fast component is always favourable for pulse shortening, it frequently cannot support self-starting mode-locking because initial (seed) long noisy pulses in the cavity fail to saturate the fast absorption. The slow temporal component in the absorption recovery is mainly responsible for start-up of the pulse operation; however, it is inefficient in short pulse shaping and requires assistance of other mechanisms, e.g. soliton formation to ensure a femtosecond pulse regime [1, 2].

In this paper we show how the specific temporal dynamics of a saturation absorber [absorber or a semiconductor saturable absorber mirror (SESAM)] influences the pulse start-up and shaping in passively mode-locked lasers. The numerical analysis developed for two-exponential absorption recovery comprising fast and slow components shows that the proper balance between fractional modulation depths and time constants can offer both the robust start of pulse generation and efficient pulse shortening. This scenario of ultrashort pulse generation is illustrated here by comparison of the bi-temporal dynamics with the recovery process involving either single-exponential fast or slow component.

O.G. Okhotnikov Optoelectronics Research Centre, Tampere University of Technology, P.O. Box 692, FIN-33101 Tampere, Finland; e-mail: oleg.okhotnikov@tut.fi;
R. Herda TOPTICA Photonics AG, Lochhamer Schlag 19, 82166 Gräfelfing, Germany

Received 13 April 2010; revision received 19 April 2011
Kvantovaya Elektronika **41** (7) 610–613 (2011)
Translated by O.G. Okhotnikov

2. Model

The simulation procedure of the passively mode-locked laser used here has been described in details elsewhere [3]. The simulation starts from the quantum noise and evolves to steady-state mode-locking. The threshold criterion for start-up of the pulse regime was chosen to be 10000 round-trips in the cavity. If the steady state is not achieved during this time period, we conclude that mode-locking is not self-starting. The time span used in numerical simulations covers the entire round-trip range, i.e. 10 ns for a repetition rate of 100 MHz. The laser model takes into account the effects critical for self-starting, particularly, the dependence of the absorber response on the pulse width, the spectral filtering induced by gain bandwidth, dispersion, self-phase modulation and the discrete location of cavity elements. Intensity-dependent phase effects are also included in the model. The slow gain dynamics typical of glass systems has been neglected [1, 4].

To avoid the influence of soliton-shaping effects usually providing the dominant pulse compression and thus limiting the role of the absorber mainly to start-up and stabilisation of the pulse regime [5], the total cavity dispersion was set to be slightly normal with the second and third order dispersion $D_2 = 0.014$ ps^2 and $D_3 = 0.0003$ ps^3, respectively. The nonlinearity in the cavity is assumed to be 5 W^{-1} km^{-1} and the round-trip cavity loss is set to 4 dB. The slow and fast components in the temporal SESAM response are defined as:

$$P_r(t) = P_i(t)[1 - q_0(t)] = P_i(t)[1 - q_{slow}(t)][1 - q_{fast}(t)], \quad (1)$$

where $P_i(t)$ is the power incident onto the absorber; $P_r(t)$ is the power reflected from the absorber; $q_{slow}(t)$ and $q_{fast}(t)$ are the fast and slow responses of the absorber; $q_0(t)$ is the modulation. The temporal dynamics of both components is described by the equation

$$\frac{dq_{slow,\,fast}(t)}{dt} = -\frac{q_{slow,\,fast}(t) - q_{0slow,\,0fast}(t)}{\tau_{slow,\,fast}} - \frac{I(t)\,q_{slow,\,fast}(t)}{E_{sat}}, \quad (2)$$

where $I(t)$ is the intensity of incident radiation; E_{sat} is the saturation energy; $q_{0\,slow}$ and $q_{0\,fast}$ are the contributions of the slow or fast component to the modulation depth; τ_{slow} and τ_{fast} are

the slow and fast recovery times, respectively. Solving equations (2) for $I(t) = 0$ and substituting these solutions into equation (1) yields an expression for a double exponential response of the absorber with fast and slow recovery components, assuming $q_{\text{slow}} \ll 1$, $q_{\text{fast}} \ll 1$:

$$P_{\text{r}}(t) = P_{\text{i}}(t)[1 - q_{0\,\text{slow}} - q_{0\,\text{fast}} + q_{0\,\text{slow}}\exp(-t/\tau_{\text{slow}}) + q_{0\,\text{fast}}\exp(-t/\tau_{\text{fast}})].$$

The slow and fast reflectivity responses of the SESAM used in the model are presented in Fig. 1 with time constant of $\tau_{\text{slow}} = 200$ ps for slow recovery component and $\tau_{\text{fast}} = 0.2$ ps for fast decay. For the two-exponential recovery dynamics the simulation uses the equal contribution of these components to the total nonlinear response of the SESAM, e.g. $\Delta R_{\text{fast}}/\Delta R_{\text{slow}} = 1$, where ΔR_{fast} and ΔR_{slow} are the fractional modulation depths of fast and slow recovery components. The saturation fluence and the modulation depth are $E_{\text{sat}} = 1$ pJ and $q_0 = 0.1$, i.e. $\Delta R_{\text{fast}} + \Delta R_{\text{slow}} = \Delta R_0 = 0.1$, where ΔR_0 is the total modulation depth of the SESAM response.

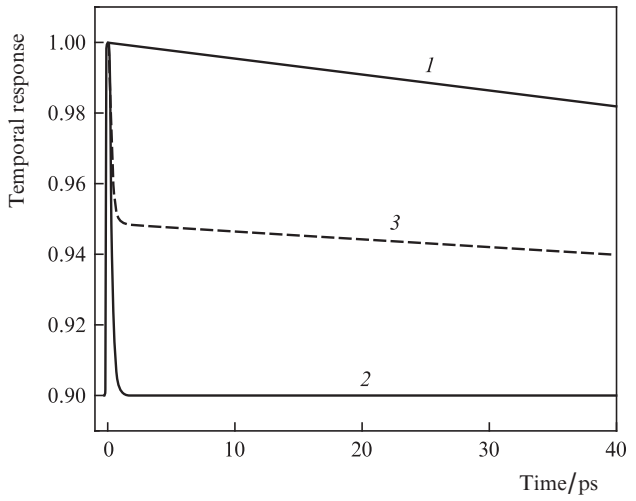

Figure 1. Temporal response of the SESAM with a slow (*1*), fast (*2*) and bi-exponential (*3*) recovery dynamics.

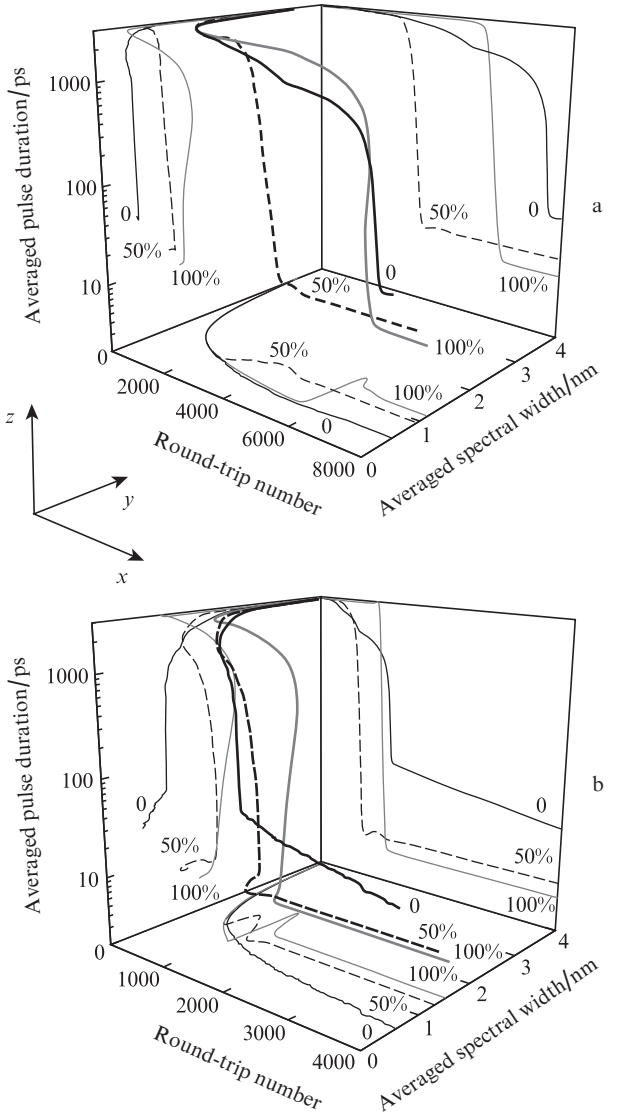

Figure 2. Pulse evolution in the pulse duration–spectral bandwidth parameter space versus the round-trip number for modulation depth of $\Delta R_0 = 3\%$ (a) and 10% (b) and a relative strength of the fast absorber component of $\Delta R_{\text{fast}}/\Delta R_0 = 0$, 50% and 100%.

3. Results and discussion

Figure 2 shows the pulse evolution during the self-starting process by displaying the 3D dependences of the pulse duration and its spectral width trajectories on the number of round-trips in the cavity. The graph also shows the projections of the trajectories onto the *xy*, *xz* and *yz* planes. The *xy* plane shows the evolution of the spectral width versus round-trip number. The spectral width evolves from the spectral width of the initial noise towards the spectral width of the steady-state pulse. The *xz* plane shows the pulse durations for each round-trip. The initial pulse duration corresponding to cw radiation is set in the modelling to one round-trip time, and it evolves towards the steady-state pulse duration. The *yz* projections show the time-bandwidth evolution, which is also a measure for the chirp of the pulse. The trajectories show an evolution of the spectral bandwidth eventually limited by the gain bandwidth of the laser material. The typical scenario of mode-locking development from spontaneous noise includes multiple-pulse regime which builds up after several hundred round-trips and exhibits strongly amplified randomly located pulses with a progressively decreasing pulse width and significant noise suppression. In the next evolution stage, the multiple pulsing converts towards a one-pulse regime when a single pulse with shortest duration, larger bandwidth and higher peak intensity starts to dominate over background. Then the pulse gradually approaches the steady-state duration and its spectral width corresponds in an optimal case to a transform-limited pulse regime.

The evolution has been simulated for different values of the modulation depth and relative strength of the slow and fast absorption recovery mechanisms. The comparison of mode-locking for absorbers with 3% and 10% modulation depths confirms that a larger nonlinear response shortens the route to the steady state and results in shorter pulses in agreement with the general theory [1, 5]. For each modulation depth, the laser demonstrates a similar behaviour versus slow-to-fast component ratio in the absorption recovery. With a purely fast absorber, labelled as a 100% curve in Fig. 2, the start-up requires many round-trips from initial noise; however, when the

pulse acquires sufficient energy, the pulse rapidly develops to the steady state. On the contrary, the slow absorber (0% curve in Fig. 2) exhibits better pulse shaping for the low-intensity fluctuations at the onset of the pulse build-up; however, it reveals insufficient potential for ultrashort pulse generation [1]. The analysis shows that the steady-state pulse regime has not been attained even after 10000 round-trips in the cavity, as seen from Fig. 2. An absorber with slow and fast components (50% curve) is found to offer an optimal trade-off between self-starting capability and pulse quality, i.e. its proximity to transform-limited pulses.

Figure 3 shows the effect of relative contribution of fast and slow recovery mechanisms $\eta = \Delta R_{\text{fast}}/(\Delta R_{\text{fast}} + \Delta R_{\text{slow}})$ on the laser performance. The steady state is considered to be achieved when the deviation $d^2 = (\sigma_t - \sigma_{t\,\text{fin}})^2/\sigma_{t\,\text{fin}}^2 + (\sigma_\lambda - \sigma_{\lambda\,\text{fin}})^2/\sigma_{\lambda\,\text{fin}}^2$ of the current values of the rms temporal (σ_t) and spectral (σ_λ) pulse widths from their rms steady-state values $\sigma_{t\,\text{fin}}$ and $\sigma_{\lambda\,\text{fin}}$ is below 0.01. The figure also shows that there is an optimum value for the relative strength of fast and slow recovery mechanisms. When the fast recovery has an excessive contribution to the total modulation depth, $\eta > 0.8$, initially long noise pulses are insufficiently shaped and experience significant losses; as a result, the start-up time of mode-locking increases dramatically. For the dominant slow recovery, $\eta < 0.35$, an initial background noise grows and becomes strong because the loss induced by the slow absorber is low at the pulse trailing edge. Eventually with an excessively long recovery time, the mode-locking becomes unstable and could reach the steady state only after many round-trips [1]. Though the behaviour for $\Delta R_0 = 3\%$ and 10% shown in Fig. 3 is qualitatively similar, we should note the positive impact of the modulation depth on the efficiency of pulse shortening.

The role of temporal characteristics of the absorber recovery is further clarified in Fig. 4 by mapping the relative pulse shortening $\Delta\tau/\tau_p$ in the pulse duration – energy parameter space achieved after one reflection from the SESAM. White background corresponds to the strong pulse shortening of ~1% as shown in the upper left corner of the Figure. The calculations have been performed for the pulse energy range from 10 pJ to 1000 pJ and pulse duration between 100 fs and 10 ns. The total modulation depth of the SESAM is kept at 0.1 for all simulations.

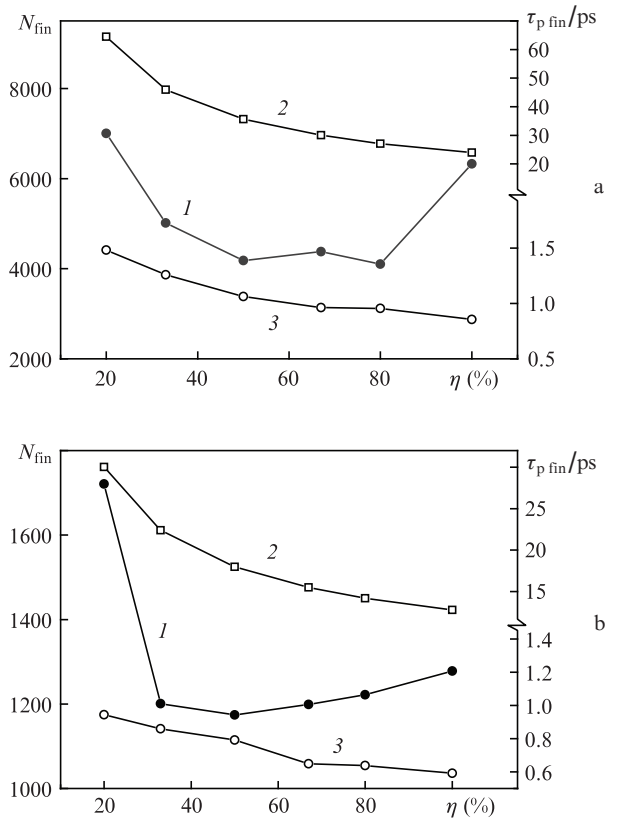

Figure 3. Results of numerical simulation representing the number of cavity round-trips required for the start-up of the mode-locked operation, N_{fin} (*1*) and steady-state pulse duration $\tau_{p\,\text{fin}}$ with a chirp (*2*) and without it (*3*) versus the relative contribution of the fast and slow components, $\eta = \Delta R_{\text{fast}}/(\Delta R_{\text{fast}} + \Delta R_{\text{slow}})$, in the absorption recovery at a modulation depth of $\Delta R_0 = 3\%$ (a) and 10% (b).

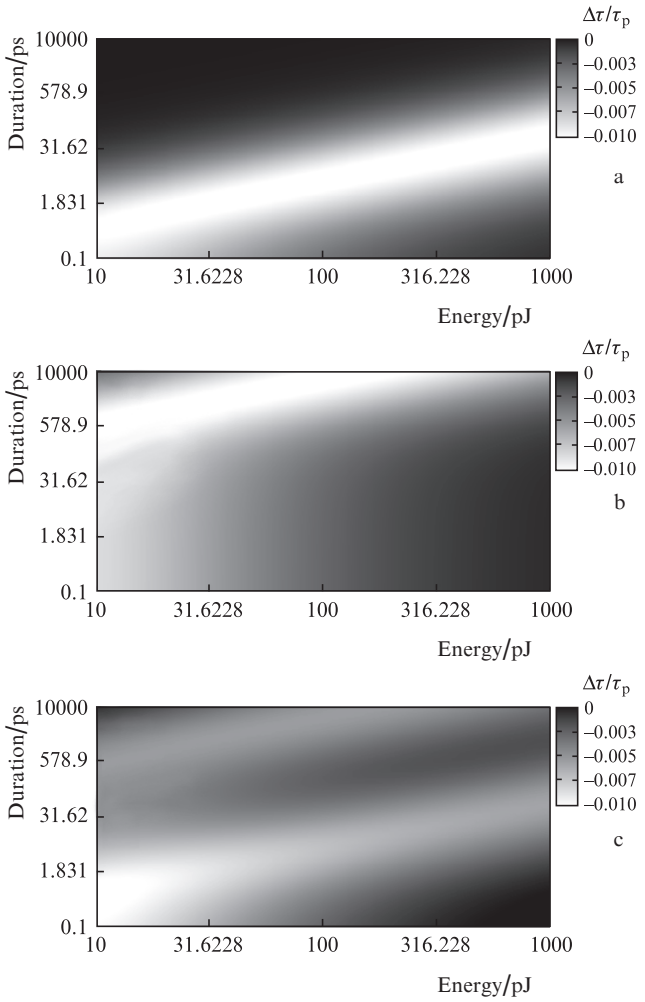

Figure 4. Pulse shortening after one reflection from the SESAM having only a fast ($\Delta R_{\text{slow}} = 0$) (a), a slow ($\Delta R_{\text{fast}} = 0$) (b) and both ($\Delta R_{\text{fast}} = \Delta R_{\text{slow}} = 0.5$) (c) recovery mechanisms. The time constants are $\tau_{\text{fast}} = 200$ fs, $\tau_{\text{slow}} = 200$ ps.

Figures 4a and b present the single-exponential recovery of the absorption corresponding to either fast or slow dynamics, respectively. The comparison of Figs 4a and b indicates that the regime of efficient pulse shortening shift towards longer pulse width when the recovery time of saturable absorption increases. The regime of efficient pulse shortening also shifts towards longer pulse widths with the pulse energy.

The analysis reveals that single recovery mechanism resulting in a single-exponential dynamics of the saturable absorber provides efficient pulse shaping only for a limited range of incident pulses. The range for the expected steady-state pulse width indicated in Figs 4a and b as a white area shifts gradually towards larger values with an increase in the pulse energy as $E_p/E_{sat} \approx 0.58\tau_p/\tau_{abs}$, where E_p/E_{sat} is the ratio of the pulse energy to the absorber saturation energy and τ_p/τ_{abs} is the ratio of the pulse duration to the absorber recovery time [6]. Particularly, this expression suggests that an absorber with the single-exponential recovery dynamics is unable to shape efficiently both long and short pulses with comparable pulse energies.

In contrast, the absorber exhibiting both slow and fast mechanisms demonstrates an enlarged parameter range of efficient pulse shortening (Fig. 4c). It is seen that a larger dynamic bandwidth of the nonlinear response of bi-temporal absorption recovery favours the pulse shaping potential for the extended range of pulse durations from subpicosecond to nanosecond. Some decrease in the relative pulse shortening per reflection from the SESAM compared with the single-exponential dynamics is observed because the total modulation depth of $\Delta R_0 = \Delta R_{fast} + \Delta R_{slow} = 0.1$ is equally shared between two recovery components.

4. Conclusions

The joint action of fast and slow relaxation mechanisms contributing to the nonlinear response of the saturable absorber is shown to have a significant impact on the mode-locking scenario. The analysis of the complex nonlinear dynamics involving relaxation processes with different speed of absorption recovery indicates that the multi-exponential recovery process would be beneficial to the performance of passively mode-locked lasers. To take a full advantage of the complex saturation decay, each dynamical constituent of the relaxation should bring in an adequate contribution to the whole nonlinear response.

References

1. Paschotta R., Keller U. *Appl. Phys. B*, **73**, 653 (2001).
2. Guina M., Xiang N., Vainionpää A., Okhotnikov O.G., Sajavaara T., Keinonen J. *Opt. Lett.*, **26**, 1809 (2001).
3. Shtyrina O., Fedoruk M., Turitsyn S., Herda R., Okhotnikov O. *J. Opt. Soc. Am. B*, **26**, 346 (2009).
4. Haus H.A. *IEEE J. Quantum Electron.*, **12**, 169 (1976).
5. Kärtner F.X., aus der Au J., Keller U. *IEEE J. Sel. Top. Quantum Electron.*, **4**, 159 (1998).
6. Hakulinen T., Herda R., Okhotnikov O. *IEEE Photonics Technol. Lett.*, **19**, 333 (2007).